CORTEX 155 (2022) 62–74

Available online at www.sciencedirect.com

ScienceDirect

Journal homepage: www.elsevier.com/locate/cortex

Single Case Report

High-density EEG power topography and connectivity during confusional arousal

Anna Castelnovo [a,b,c,*,1], Julian Amacker [d,1], Massimo Maiolo [d,e], Ninfa Amato [a], Matteo Pereno [a], Silvia Riccardi [a], Andrea Danani [f], Simone Ulzega [d] and Mauro Manconi [a,b,g]

[a] Sleep Medicine Unit, Neurocenter of Southern Switzerland, Ospedale Civico, Lugano, Switzerland
[b] Faculty of Biomedical Sciences, University of Southern Switzerland, Lugano, Switzerland
[c] University Hospital of Psychiatry and Psychotherapy, University of Bern, Bern, Switzerland
[d] Institute of Computational Life Sciences, Zurich University of Applied Sciences, Wädenswil, Switzerland
[e] Institute of Pathology, University of Bern, Bern, Switzerland
[f] Dalle Molle Institute for Artificial Intelligence, USI-SUPSI, Lugano, Switzerland
[g] Department of Neurology, University Hospital, Inselspital, Bern, Switzerland

ARTICLE INFO

Article history:
Received 20 February 2022
Reviewed 25 April 2022
Revised 28 April 2022
Accepted 29 May 2022
Action editor Veena Kumari
Published online 22 July 2022

Keywords:
Disorders of arousal
NREM-sleep parasomnia
Somnambulism
Night terror
Pavor nocturnus

ABSTRACT

Confusional arousal is the milder expression of a family of disorders known as Disorders of Arousal (DOA) from non-REM sleep. These disorders are characterized by recurrent abnormal behaviors that occur in a state of reduced awareness for the external environment. Despite frequent amnesia for the nocturnal events, when actively probed, patients are able to report vivid hallucinatory/dream-like mental imagery. Traditional (low-density) scalp and stereo-electroencephalographic (EEG) recordings previously showed a pathological admixture of slow oscillations typical of NREM sleep and wake-like fast-mixed frequencies during these phenomena. However, our knowledge about the specific neural EEG dynamics over the entire brain is limited.

We collected 2 consecutive in-laboratory sleep recordings using high-density (hd)-EEG (256 vertex-referenced geodesic system) coupled with standard video-polysomnography (v-PSG) from a 12-year-old drug-naïve and otherwise healthy child with a long-lasting history of sleepwalking. Source power topography and functional connectivity were computed during 20 selected confusional arousal episodes (from −6 to +18 sec after motor onset), and during baseline slow wave sleep preceding each episode (from − 3 to −2 min before onset).

We found a widespread increase in slow wave activity (SWA) theta, alpha, beta, gamma power, associated with a parallel decrease in the sigma range during behavioral episodes

Abbreviations: BEM, Boundary Element Model; DOA, Disorders of Arousal; EEG, Electroencephalography/ic; FDR, False-discovery rate; NREM, Non-rapid eye movement; PSD, Power Spectral Density; PTE, Phase Transfer Entropy; RDI, Respiratory Disturbance Index; SHE, Sleep-related hyper-motor epilepsy; sLORETA, Standardized low resolution electromagnetic tomography; PLMSI, Periodic Limb Movements Index during Sleep; SPECT, Single photon emission computed tomography; SWA, Slow Wave Activity; vPSG, Video-polysomnography.

* *Corresponding author*. Via Tesserete 46, 6900 Lugano,
E-mail address: anna.castelnovo@eoc.ch (A. Castelnovo).
[1] These two authors contributed equally to the manuscript.

https://doi.org/10.1016/j.cortex.2022.05.021

compared to baseline sleep. Bilateral Broadman area 7 and right Broadman areas 39 and 40 were relatively spared by the massive increase in SWA power. Functional SWA connectivity analysis revealed a drastic increase in the number and complexity of connections from baseline sleep to full-blown episodes, that mainly involved an increased out-flow from bilateral fronto-medial prefrontal cortex and left temporal lobe to other cortical regions. These effects could be appreciated in the 6 sec window preceding behavioral onset.

Overall, our results support the idea that DOA are the expression of peculiar brain states, compatible with a partial re-emergence of consciousness.

1. Introduction

DOA are Non-Rapid Eye Movement (NREM) sleep parasomnias that are thought to derive from incomplete arousal out of NREM sleep (Castelnovo, Lopez, Proserpio, Nobili, & Dauvilliers, 2018; Zadra, Desautels, Petit, & Montplaisir, 2013). Indeed, DOA episodes are characterized by recurrent abnormal sleep-related complex behaviors, lasting from a few seconds to several minutes, associated with various degrees of autonomic activation, and inappropriate or scarce responsiveness to the external environment. These behaviors may range from sitting in the bed quietly with the eyes usually wide open (confusional arousal) to screaming loudly and other fear-related expressions (night terrors) and/or wandering about in the house or even outdoor (sleepwalking). Patients are often amnestic for their events, but when actively probed they may report vivid mental images, thoughts and emotions that are evocative of an hallucinatory/dreaming state (Baldini et al., 2019; Castelnovo, Loddo, Provini, & Manconi, 2021; Castelnovo, Loddo, Provini, Miano, & Manconi, 2021; Mwenge, Brion, Uguccioni, & Arnulf, 2013; Oudiette et al., 2009; Rocha & Arnulf, 2020; Uguccioni et al., 2013).

Severe cases are associated with sleep fragmentation, daytime sleepiness, psychological distress and even with self-harm or legal consequences (Ingravallo et al., 2014). Nonetheless, little progress was made in the last decades in our understanding of DOA neurobiological underpinnings. As a consequence, the diagnosis of these complex manifestations relies solely on clinical criteria.

Sparse evidence suggested that EEG changes precede by a few seconds DOA abnormal behaviors (Desjardins et al., 2017; Espa, Ondze, Deglise, Billiard, & Besset, 2000; Guilleminault, Poyares, Abat, & Palombini, 2001; Jaar, Pilon, Carrier, Montplaisir, & Zadra, 2010; Januszko et al., 2016; Perrault, Carrier, Desautels, Montplaisir, & Zadra, 2014; Terzaghi et al., 2009; Zadra & Nielsen, 1998). Moreover, according to some old qualitative studies based on visual inspection (Schenck, Pareja, Patterson, & Mahowald, 1998; Zadra, Pilon, Joncas, Rompré, & Montplaisir, 2004), as well as quantitative evidence based on one SPECT case report (Bassetti, Vella, Donati, & Wielepp, 2000) and few stereo-EEG case report/series, DOA episodes are states of dissociation characterized by an abnormal coexistence of local sleep-like and wake-like features (Bassetti et al., 2000; Flamand et al., 2018; Sarasso et al., 2014; Terzaghi et al., 2009, 2012). Despite offering remarkable insights, all these studies suffer from limitations connected to the technique they used to investigate these phenomena. More specifically, SPECT low temporal resolution does not allow study of the temporal dynamics of DOA episodes, while stereo-EEG spatial resolution is constrained by the location of the suspected epileptogenic focus. High-density (hd)-EEG is a well-established modern technique that combines the high temporal definition of EEG, with a reasonably high spatial resolution derived by the high-number of scalp electrodes. Interestingly, a first high-density (hd) EEG case report of DOA was reported by our group, which suggested the potential role of the right hemisphere in gating the spreading of abnormal slow wave activity over the left hemisphere, mediating the occurrence of full-blown clinical episodes (Ratti, Amato, David, & Manconi, 2018).

The current work aimed at mapping the EEG dynamics prior and during clinical episodes, at both the scalp and source level, applying spectral and connectivity analyses to 2-night sleep hd-EEG recordings from a single patient with DOA.

2. Case report

2.1. *Clinical history*

The patient is a 12-year-old, Caucasian, right-handed male with a history of DOA - sleepwalking and confusional arousal sub-types (ICSD-3) since the age of 4 years. During his typical sleepwalking episodes, usually about 30–90 min after sleep onset, he quietly wandered around the house with a vacant expression and was apparently unresponsive to his parents. Less frequently, he approached his parents anxiously, mumbling or yelling complex, out-of-context, agitated statements like "You know it, oh, you know it very well!" He usually returned to bed spontaneously or guided by his parents after 1–5 min, falling back to sleep immediately. During minor confusional arousal episodes, he sat up on his bed for few seconds (<1 min), staring at the air or looking around, more often calling his sister and/or talking to her (e.g., "We are trapped in here!") and pointing to non-existent objects in the room. He was usually amnestic for the events, although during the clinical interview he was able to recall 3 episodes associated with dreamlike mental imagery (Castelnovo, Loddo, Provini, Miano, & Manconi, 2021). The family history was positive for NREM sleep parasomnias. The frequency of the episodes had been stable over the years - on average 2–3

major sleepwalking episodes per week and minor episodes almost every night. His personal medical history was unremarkable. Except for frequent sleep-talking and sleep hyperhidrosis, his sleep history was not evocative of any other sleep disorder. Medical and neurologic physical examination showed no abnormalities. Routine hematology testing was normal. The Child Behavior Checklist (Nakamura, Ebesutani, Bernstein, & Chorpita, 2009) did not reveal any behavioral or emotional problem (total score = 11, none of the subscales scored above the pathological threshold). Legal copyright restrictions prevent public archiving of the Child Behavior Checklist, which can be obtained from the copyright holder in the associated reference. Video-Polysomnography (v-PSG) monitoring was planned to exclude mimics or comorbidities. The patient was enrolled in the context of a larger observational, single-center study carried out at the Neurocenter of Southern Switzerland. All study procedures were reviewed and approved by the local Independent Ethics Committee "Comitato Etico Cantonale" (2017-01788 – n.3282, approval date: 15.12.2017), according to the regulatory requirements of Switzerland. The child and his parents provided written consent prior to the beginning of the study.

2.2. *v-PSG recording*

The patient underwent 2 overnight in-laboratory sleep recordings at the Sleep Medicine Unit of the Neurocenter of Southern Switzerland. A full montage with traditional video-PSG channels (electro-oculogram, electromyogram of the submentalis muscle and of the right and left tibialis anterior muscles, electrocardiogram, oral and nasal airflow thermistors, nasal pressure cannula, and wearable piezo-electric bands for thoracic and abdominal movements) was coupled with a high-density EEG system (256 channels; Electrical Geodesics Inc., Eugene, OR, vertex referencing, sampling rate of 500 Hz). Lights-out and light-on were within 1 h of the participant's most consistently reported bedtime. Sleep staging was performed by a board-certified sleep physician, according to standard AASM (Berry et al., 2020) criteria using the EMBLA-RemLogic software based on 30-s epochs for 6 EEG derivations extracted from the high-density EEG system, with bipolar re-referencing (F3/M2, F4/M1, C3/M2, C4/M1, O1/M2, O2/M1), EOG, and submental EMG.

Supplementary video related to this article can be found at https://doi.org/10.1016/j.cortex.2022.05.021

Sleep-disorder breathing (RDI <1) and periodic limb movements (PLMSI <5) were ruled out by concurrent v-PSG. DOA episodes were selected according to the following inclusion/exclusion criteria, which were established before data analysis: 1) episodes must be scored in line with international criteria (Berry et al., 2020) and characterized according to motor video-patterns (Loddo et al., 2018); 2) episodes must not be associated with Mayor Body Movements, as defined by international criteria (Berry et al., 2020); 3) to increase the accuracy and consistency of the evaluation of minor DOA episodes, an episode could only be retained when classified as confusional arousal by 3 independent raters looking at v-PSG, or when an agreement between the raters could be reached after discussion. Twenty behavioral events during sleep stage 3 (9 and 11 per night, respectively) were double-blindly identified by 3 different sleep medicine experts (AC, SR, MM). Episode onset was defined as an abrupt, at least-twofold amplitude increase in EMG channels (the first between chin EMG, arm EMG or leg EMG). All episodes were characterized by non-stereotyped motor behaviors - type I and type II patterns (Loddo et al., 2018). Behaviors ranged from head flexion/extension, limb movements or partial trunk flexion/extension in variable combinations to a complete trunk flexion with patient sitting up in bed with a blind gaze or looking around (see Supplementary Material for an explicative Videoclip). Some episodes were associated with partially intelligible speech. Episodes lasted from about 15 to 30 sec. After episodes, the patient rapidly fell asleep again except for a couple of longer episodes ending with a brief confusional phase and a progressive re-emergence into wakefulness. The subsequent morning the patient did not recall any of the events.

2.3. *Hd-EEG data analysis*

EEG data analysis was conducted with MATLAB (Mathworks Inc., Natick, MA, USA) using the EEGLAB v13 (Delorme & Makeig, 2004) and BRAINSTORM (Tadel, Baillet, Mosher, Pantazis, & Leahy, 2011) toolboxes, and custom scripts. Recordings were off-line high-pass filtered (.1 Hz IIR filter reproducing a single resistor capacity), and subsequently band-pass filtered (.5–45 Hz, Kaiser window-based FIR with zero-phase distortion). From the all-night hd-EEG recordings, segments commencing 3 min before and ending 1 min after each episode onset were selected for further analysis. Data channels and segments containing artifactual activity were visually identified and marked as bad using the BRAINSTORM graphical interface. The signal was then re-referenced to the average of the scalp voltage for all 256 channels. Bad epochs were rejected and the signal for bad channels was reconstructed from the weighted average of neighboring channels using spherical interpolation and with a maximal distance between electrodes of 5 cm.

Source modeling was performed with Brainstorm using an age-appropriate template (Richards, Sanchez, Phillips-Meek, & Xie, 2016), segmented using SPM12/CAT12 Matlab toolbox (Tzourio-Mazoyer et al., 2002). A symmetric BEM of the head having three realistic layers (scalp, inner skull, outer skull) (Maureen, 2010) and a standard co-registered set of electrode positions were used to construct the forward model. The inverse matrix was computed using the sLORETA Minimum Norm (Pascal-Marqui, 2002) with sources constrained to be perpendicular to the cortical surface and retaining only diagonal elements of the noise covariance matrix.

PSD was computed at the scalp level and in source space using Welch's modified periodogram method in 6-s Hamming windows with 50% overlap. The magnitude of the complex PSD was extracted for further analysis. The primary analysis focused on average magnitude of PSD in the .5–4 Hz range, which is associated with slow waves (SWA). A subsequent analysis then explored between-state differences in oscillatory power in theta (4–8 Hz), alpha (8–12 Hz), sigma (12–16 Hz), beta (18–30 Hz) and low gamma (30–45 Hz) frequency bands. For the scalp level both absolute average referenced and subject-normalized (using z-score across

channels) topographic maps were examined, while in source space only the normalized maps (using sLORETA based minimum norm estimates) were considered.

Moreover, Phase Transfer Entropy (PTE) (Lobier, Siebenhühner, Palva, & Palva, 2014), a measure of directed connectivity among neuronal oscillations, was computed at the source level using the average source activity in brain regions defined by the Destrieux atlas for cortical parcellation (Destrieux, Fischl, Dale, & Halgren, 2010). The PTE was normalized according to Hillebrand et al., 2016 (Hillebrand et al., 2016).

The use of PTE as a metric for functional connectivity analysis has several benefits over other methods, namely, it is not biased by artificial zero-lag correlations and it allows interference in the connectivity phase coupling directionality (Hillebrand et al., 2016; Lobier et al., 2014). Thus, PTE is an excellent exploratory method as it does not make any assumptions about the data. Moreover, PTE can detect nonlinear directed information flows, unlike other coherence-based methods, and thus emerges as a very well-suited approach to infer multiple-pathway functional connectivity patterns, typical of brain networks.

Two behavioral states were selected: baseline stage 3 sleep (−180 to −120 sec before onset) and DOA events (from −6 to + 18 sec). DOA events were further subdivided into 3 time-windows: 1) pre-episode (−6 sec from onset to onset), episode T1 (from onset to 6 sec after onset), episode T2 (from 6 to 12 sec from onset), and episode T3 (from 12 to 18 sec from onset). Six-second windows were chosen on the basis of a stereo-EEG study that captured EEG activity changes 5 sec before the start of the clinical onset (Terzaghi et al., 2009) – and to ensure the stability of connectivity results (Fraschini et al., 2016).

Statistical comparisons for sensor and source topographical analysis were made within-subjects and used 2-sided paired t-tests between behavioral states. Group level analyses on the average PSD values were performed separately for each frequency band. Whole cortex analyses were conducted correcting for multiple comparisons using a nonparametric cluster based permutation test (Nichols & Holmes, 2001) with 10000 permutations for scalp power topography and using topological cluster false-discovery rate (FDR) for source power topography and connectivity. Cluster-size tests were used to test for significant regions using a cluster-forming threshold of $p = .05$ and a cluster size threshold of $p < .05$ (cluster corrected).

3. Results

Scalp power analysis. Pre-episode, compared to baseline, was associated with a widespread significant increase in absolute power in SWA. At an exploratory analysis, a similar increase involved theta (Fig. 1, column 1). Normalized maps displayed a significant cluster of relative decrease in sigma and a pattern of relative decrease over frontal areas in lower frequency bands (Supplementary Figure 1, column 1). Episode T1, compared to baseline, was associated with a diffuse increase of absolute power in all frequency bands (Fig. 1, column 2), which decreased over time for lower frequencies in Episode T2 and T3 (Fig. 1, column 3 and 4). The only exception was sigma, which

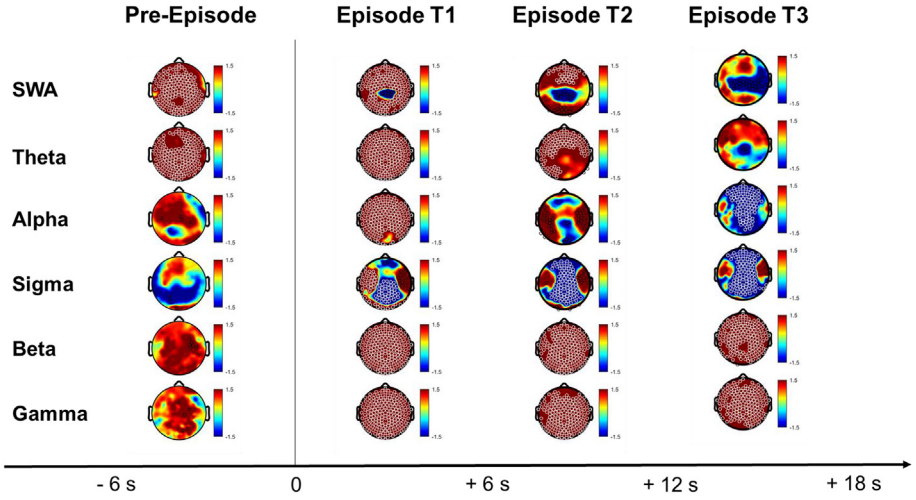

Fig. 1 – Scalp power analysis in all frequency bands. Rows: frequency bands of interest as indicated: SWA (.5–4 Hz), theta (4–8 Hz), alpha (8–12 Hz), sigma (12–16 Hz), beta (18–25 Hz), gamma (25–45 Hz). Columns: comparison between absolute power at baseline and pre-episode, episode T1, episode T2, episode T3. The horizontal black arrow at the bottom defines time in seconds. Baseline: average power from −3 to −2 min before behavioral onset. Pre-episode (column 1): average power from −6 sec prior to onset to onset. Episode T1 (column 2): from onset to 6 sec after onset. Episode T2 (column 3): from 6 to 12 sec after onset. Episode T3 (column 4): from 12 to 18 sec after onset. Blue values: a decrease in absolute EEG power in pre-episode relative to baseline (pre-episode < baseline). Red values: an increase (pre-episode > baseline). White dots: channels that belong to a statistically significant cluster of electrodes ($p \leq .05$) using statistical nonparametric mapping suprathreshold cluster testing. Black dots: individual channels with $p < .05$ (uncorrected). Note: Electrodes on the face and outer ring of the sensor net were eliminated entirely for all participants due to excessive artifacts, yielding a final scalp montage of 186 channels.

displayed a stable decrease over midline brain regions, with a distribution resembling sleep spindle topography in both absolute and normalized power maps (Fig. 1, column 2 to 4).

Of note, in the SWA range, a central cluster of channels was spared by the global power increase (Fig. 1, column 2). This effect became progressively more accentuated over time (Fig. 1, column 3 and 4) and emerged more clearly in normalized maps (Supplementary Figure 1, column 4, 6 and 8). A similar pattern could also be observed in normalized theta values, with a more accentuated antero-posterior discrepancy (Supplementary Figure 1, column 2 to 4).

Cortical source power analysis. No significant differences in band power between pre-episode and baseline were observed in any frequency band at the source level (Fig. 2, column 1). Relative higher SWA power could be observed at the beginning of the episodes (T1) in almost all brain regions except for a centro-posterior zone mainly represented by the precuneus and the superior parietal lobe, bilaterally (Fig. 2, column 2). This increased activity could still be observed mainly over the left hemisphere at T2 in the orbital frontal cortex and gyrus rectus, temporal pole, the anterior, mid and ventral posterior cingulate, the insula, and occipital visual areas (inferior and superior occipital gyri, occipital pole) (Fig. 2, column 3), but not in later stages of the episodes (T3) (Fig. 2, column 4). Compared to baseline, Episode T3 was associated with significantly lower SWA over the right supramarginal and angular gyri, bilateral precuneus (right > left), bilateral paracentral lobule and superior parietal lobule (Fig. 3, column 4).

Exploratory comparisons for other frequency bands are summarized in Supplementary Figure 2, Supplementary Figure 3 and Supplementary Figure 4. Shortly, theta showed a pattern similar to delta, alpha and sigma displayed a relative decrease over midline brain structures and a relative increase over lateral regions, which remained stable over time (from T1 to T2). Finally, beta and gamma source power values were globally and stably increased compared to baseline (from T1 to T2).

3.1. *Connectivity analysis*

The PTE analyses in the SWA range during baseline sleep (Fig. 3A) revealed a rather simple, stereotyped and poorly differentiated pattern of connectivity where almost all information stemmed from 3 main frontal hubs (right middle and inferior frontal gyri > right orbito-lateral frontal cortex > left middle and inferior frontal gyri) and was directed towards almost all brain regions. A disruption of this pattern could be already observed in the pre-episode period (Fig. 3B) that

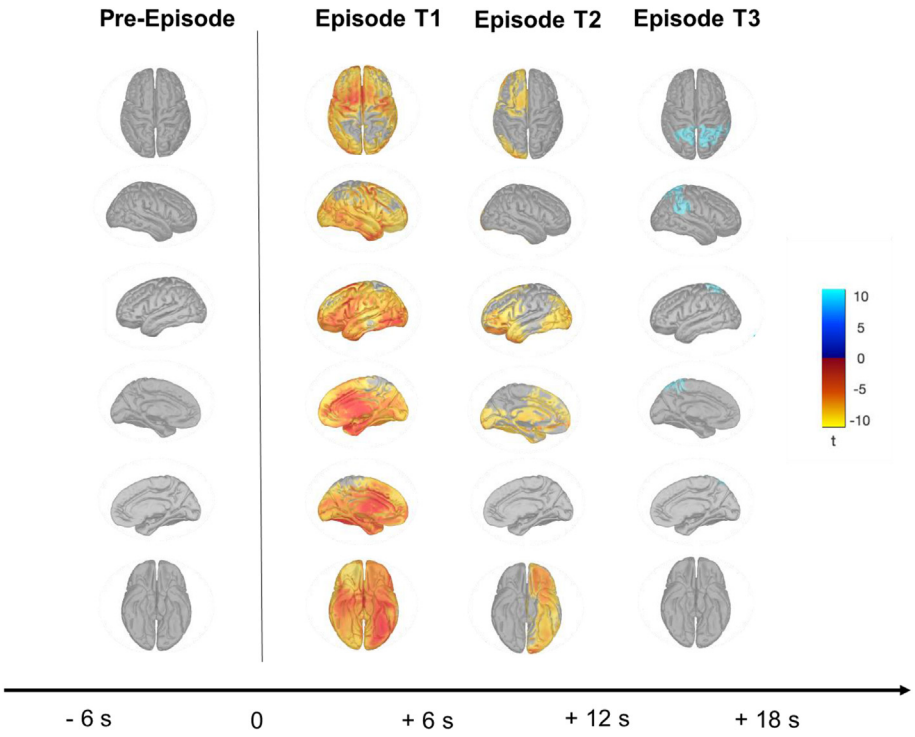

Fig. 2 – SWA source power analysis. Columns: comparison between absolute power at baseline and pre-episode, episode T1, episode T2, episode T3. The horizontal black arrow at the bottom defines time in seconds. Baseline: from −3 to −2 min before behavioral onset. Pre-episode: from −6 sec prior to onset to onset. Episode T1: from onset to 6 sec after onset. Episode T2: from 6 to 12 sec after onset. Episode T3: from 12 to 18 sec after onset. Gray color: non-significant differences after correction for multiple comparison using topological cluster false-discovery rate (FDR). Blue color: a significant decrease in source power in pre-episode or episode relative to baseline (pre-episode/episode < baseline) using FDR. Red color: a significant increase in source power in episode relative to baseline (pre-episode/episode > baseline) using FDR. First row: Horizontal plane (top); second row: sagittal plane, right hemisphere (lateral), third row: sagittal plane, left hemisphere (lateral), fourth row: sagittal plane, right hemisphere (medial), fifth row: sagittal plane, left hemisphere (medial), sixth row: horizontal plane (bottom).

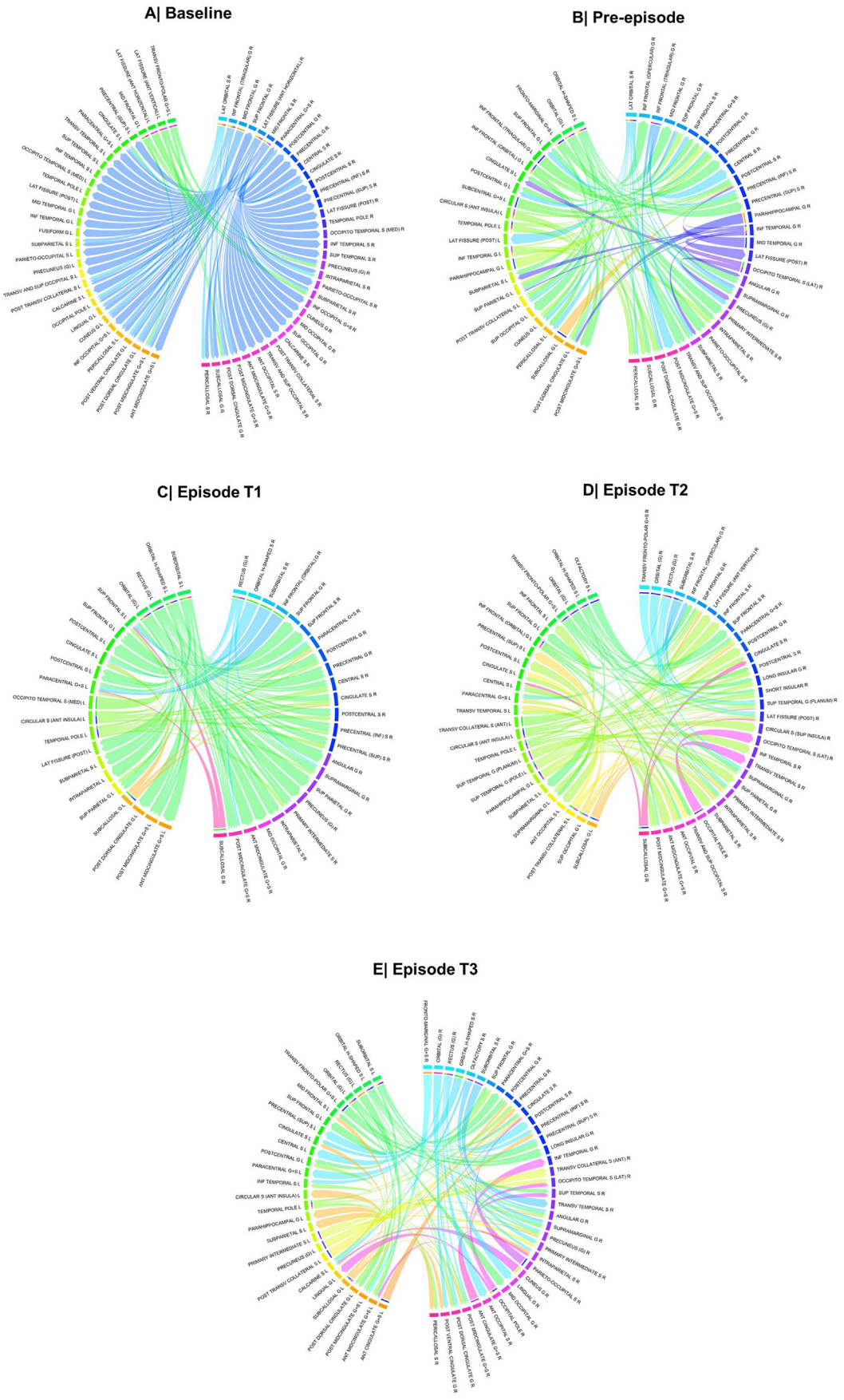
A| Baseline
B| Pre-episode
C| Episode T1
D| Episode T2
E| Episode T3

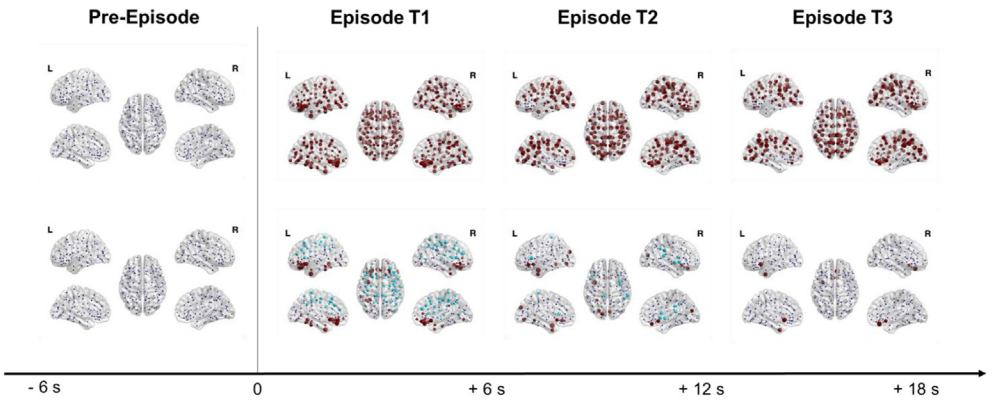

Fig. 4 – Hd-EEG source connectivity analysis (3D representation of mean strength connectivity for each brain region). Columns: comparison between outflow-inflow functional connectivity at baseline and pre-episode, episode T1, episode T2, episode T3. The horizontal black arrow at the bottom defines time in seconds. Baseline: from −3 to −2 min before behavioral onset. Pre-episode: from −6 sec prior to onset to onset. Episode T1: from onset to 6 sec after onset. Episode T2: from 6 to 12 sec after onset. Episode T3: from 12 to 18 sec after onset. Upper rows: statistical comparison of global PTE connectivity (sum of input and output) in each brain region/node. Bottom rows: statistical comparison of global PTE connectivity (different of input and output) in each brain region/node.

displayed a more scattered, integrated and differentiated network of connections originating mainly from: (i) the left temporal lobe: left anterior insula, left temporal pole, left parahippocampal gyrus > (ii) the left frontal lobe (with hubs distributed more anteriorly than during baseline): left orbito-frontal cortex and left gyrus rectus, left orbito-lateral frontal sulcus and to a lesser extent left inferior frontal gyrus (orbital and triangular part) > (iii) the right temporal lobe: lateral inferior, middle and superior temporal gyri as well as para-hippocampal gyrus > (iv) right orbito-lateral frontal sulcus and right inferior temporal lobe (triangular part).

During the episode, PTE connectivity hubs involved the entire orbitofrontal cortices, bilaterally, the left temporal pole, while the right temporal lobe hub was progressively lost, with the concomitant emergence of more scattered connections over parieto-occipital bilateral brain regions (Fig. 3C D and E).

Absolute SWA connectivity (sum of input and output connections from each brain area) was globally increased in pre-episode and during the episode compared to baseline (Fig. 4, upper rows), while net connectivity (meaning the difference between output and input) basically reflected what described for circular plots (Fig. 4, lower rows). At the very beginning of the episode there was a bilateral higher outflow of information from left and right orbitofrontal and inferior lateral frontal brain regions as well as polar and infero/medial temporal areas, and a higher inflow in almost all other brain regions compared to baseline. Subsequently, the increase in outflow persisted bilaterally over basal frontal regions but was skewed towards the left temporal lobe while the increase in inflow displayed the opposite effect.

4. Discussion

This is the first study investigating broad-band brain EEG scalp/source power topography and connectivity prior to and during clinical DOA episodes using hd-EEG, which allowed for a precise analysis of local changes in the space and time domains.

20 confusional arousal episodes (from −6 sec before to + 8 sec after motor onset) were extracted from 2-night recordings in the same subject (a 12-year-old male). The hd-EEG activity in 4-time windows (pre-episode: −6 to 0 sec, episode t1: 0 to + 6 sec, episode t2: from +6 to +12 sec, episode t3: +12 to +18 sec) was extracted and compared to stable slow wave sleep (baseline: −2 to −3 min before onset).

At the scalp level, we found a widespread increase of scalp SWA and theta in pre-episode compared to baseline and an increase in SWA, theta, alpha, beta, gamma, associated with a parallel decrease in sigma during episode compared to baseline. Notably, the increase in SWA power displayed a specific regional pattern that spared bilaterally Broadman area 7 and right Broadman areas 39 and 40.

Functional connectivity in the SWA range underwent drastic changes from pre-episode to episode compared to baseline, with a significant increase in the number and in the distribution of connections. Importantly, the key areas implicated seemed to be the frontal lobes (mainly right infero-lateral prefrontal cortex during baseline and bilateral ventro-medial pre-frontal cortex during clinical episodes) and the left anterior insula/left anterior temporal lobe (mainly infero-

Fig. 3 – Hd-EEG SWA source functional connectivity analysis (circular plots). Circular plots for average functional connectivity (PTE: phase transfer entropy) at A) Baseline: from −3 to −2 min before behavioral onset, B) Pre-episode: from −6 sec prior to onset to onset, C) Episode T1: from onset to 6 sec after onset, D) Episode T2: from 6 to 12 sec after onset, E) Episode T3: from 12 to 18 sec after onset. The direction of the arrow indicates the direction of functional connectivity. Ant: anterior. Post: posterior. Sup: superior. Inf: Inferior. Transv: transverse. G: gyrus. S: Sulcus. L: left. R: right.

lateral, ventral and medial). Overall, during DOA episodes compared to baseline sleep, connectivity seemed to mainly flow from ventral to dorsal, and from left to right brain areas.

4.1. *Comparison with the literature*

Our power results for pre-episode versus baseline are in line with the sparse existing literature, add relevant topographic information and support a consistency of findings in children, previously investigated only by Espa et al. (2000).

At the turn of last century, Zadra and Nielsen reported for the first time a specific increase in SWA prior to night terrors from a single subject compared to average slow wave sleep from a control group (Zadra & Nielsen, 1998). This effect was larger over fronto-central channels and asymmetrically distributed (left > right, 19 channel montage). Subsequently, 4 studies conducted on small groups of patients with sleepwalking and/or sleep terrors (n = 11–22), confirmed an increase in SWA at central or midline leads, with some discrepancies related to the pattern of increase: a progressive increase over the preceding several minutes in a group of children (Espa et al., 2000) versus a clear-cut increase in the few preceding (from 30 to 12) seconds in adults (Desjardins et al., 2017; Guilleminault et al., 2001; Jaar et al., 2010).

The parallel increase in theta prior to episodes compared to baseline was previously described by Desjardins at al., who reported an increase in delta and theta (but not in alpha and beta) in the 20 sec preceding episodes compared to baseline (n = 27, 3 midline leads).

Sigma power - which indirectly represents sleep spindles - tended to decrease just prior to DOA episodes compared to baseline, although at a non-significant level, once again in line with a previous observation of a trend-significance by Desjardin et al. (Desjardins et al., 2017). In our case, the decrease was localized in a central parietal cluster of electrodes resembling the typical distribution of fast spindles.

Finally, beta and gamma tended to be higher in pre-episode versus baseline, reaching significance in the 2-s window prior to onset (data not shown). To the best of our knowledge, gamma activity has not been reported by previous studies, while Januszko et al. found a similar increase in high beta (24–30 Hz), localized at the level of the cingulate motor area when comparing −8 to −4 sec segments to −4 sec to onset segments (Januszko et al., 2016).

At the source level, no significant difference emerged in the power maps of any frequency band during the pre-episode compared to baseline. The only previous hd-EEG study (Ratti et al., 2018) – a case report on a young man suffering from sleepwalking – found an increase of low SWA power in the 5 sec prior to behavioral onset in the right prefrontal cortex (Brodmann's areas 10 and 11). The instability of source findings in the pre-episode period might be related to the different definition of behavioral onset: in the current case report, it was defined as the first EMG movement of chin, legs, or arms, while the previous case report only used chin EMG.

Subsequently, during DOA episodes, absolute SWA power remained globally higher compared to baseline at the scalp level and this effect also turned out to be significant at the source level. Moreover, source analysis revealed a specific regional pattern, not previously described, where parietal higher order associative brain regions (bilateral precuneus and paracentral lobules and right temporo-parieto-occipital junction) were relatively spared by an overwise widespread increase. The previously mentioned hd-EEG case report by Ratti et al. also reported that SWA power, after an initial increase over the right prefrontal cortex just prior to behavioral onset, spread bilaterally and involved the left prefrontal and left temporal cortices in the 0 to 10 sec-span after onset (Ratti et al., 2018). These areas displayed the maximal increase in SWA power in our current analysis. However, Ratti et al. could not detect areas of local relative decrease in SWA power, probably because this latter finding emerged progressively and became significant only between 12 and 18 sec after onset, a time-window not previously investigated. Of note, from 6 to 12 sec after onset, we only found a lateralized effect over the left hemisphere, as in Zadra et al. (Zadra & Nielsen, 1998). Despite the interesting possibility that inter-hemispheric asymmetry plays a role in the development of clinical DOA episodes, the degree of lateralization may vary in different episodes or in different patients.

The scalp and source analysis of other frequency bands during DOA episodes (after behavioral onset) is novel and therefore can't be compared to previous works. It yielded a significant, stable absolute decrease in sigma during DOA episodes compared to baseline, and an absolute increase in theta, alpha, beta and gamma. This increase remained constant throughout the episodes for beta and gamma, while it progressively disappeared for theta and alpha. Beta and gamma were less interpretable because of possible temporal and neck muscle artifacts. However, even considering this limitation, it is interesting to note that central channels (with no artifacts) showed a diffuse increase in high frequencies both at the source and scalp level.

To the best of our knowledge, no previous work investigated EEG connectivity during DOA episodes. Only one study explored connectivity prior to DOA episodes using the imaginary part of the coherence over a longer period of time (20 sec) prior to episode onset, compared to the 20 sec of baseline slow wave sleep occurring 2 min before the episodes (Desjardins et al., 2017). This work revealed a decrease in delta EEG functional connectivity in parietal and occipital regions and in increase of long-range connectivity in alpha and beta range. The use of the imaginary part of coherence (Nolte et al., 2004), as opposed to methods such as Coherency or Phase Locking Value, for evaluating phase coupling between signals, allows circumvention of artificial zero-lag correlations, such as those induced by source leakage (volume conduction problem). However, in general all methods based on coherence estimates, contrary to nonlinear measures of frequency dependence, such as PTE, can be affected by changes in amplitude. Therefore, phase correlated channels, which are not correlated in amplitude, may be lost using a coherence-based approach (Greenblatt, Pflieger, & Ossadtchi, 2012; Pereda, Quiroga, & Bhattacharya, 2005).

4.2. *Interpretation of results*

Current power results during the pre-episode period share similarities with known EEG modifications prior to physiological arousal. More specifically, an increase in fronto-central

SWA and theta activities was previously observed during the 2 sec before arousal onset (Sforza, Jouny, & Ibanez, 2000). Moreover, arousal is known to be associated with a blockage of sleep spindles (Naitoh, Antony-Baas, Muzet, & Ehrhart, 1982; Peter-Derex, Magnin, & Bastuji, 2015), which have been connected with the preservation of sleep continuity (Fernandez & Lüthi, 2020).

The aforementioned similarities between the pre-arousal period and pre-DOA period, on one hand, support a common background, and on the other hand raise concerns about where, when, and how a physiological arousal response becomes dysfunctional in patients with DOA. To date, only 2 studies, based on a limited number of patients ($n = 11–12$) and channels (C3 and/or C4) explored differences between arousals and DOA episodes. These studies found greater SWA and slow oscillation density prior to DOA episodes compared to NREM arousals (Espa et al., 2000) or non-behavioral awakenings (Perrault et al., 2014). However, it remains unclear whether the difference is only related to a different degree of motor activation, as these studies did not make a distinction between motor and non-motor arousals/awakenings. In this regard, our results suggest that an initial arousal-like pattern during pre-DOA episodes later on evolves into a highly disrupted state, different from physiological arousal, leaving our patient "trapped" in a state between sleep and wakefulness. Indeed, while sigma power decreased over a centroparietal cluster of electrodes as during N3 arousal (Peter-Derex et al., 2015), all other frequency bands showed an effect in the opposite direction, meaning a massive global increase. This effect could not be observed during N3 arousal based on the limited available literature. More specifically, a stereo-EEG study (Peter-Derex et al., 2015) detected an overall decrease in delta power in all recorded cortical areas in about 60% of the cases, no changes in the majority of the remaining cases, and a rare paradoxical increase in high-amplitude rhythmic slow wave activity (mainly in frontal but also in parietal dorsolateral cortices). An interesting, although yet speculative hypothesis, could be that DOA episodes arise from an exaggeration or/and an abnormal distribution and persistence of this latter physiological SWA activity.

Taken together, our broad-spectrum power results support the notion of an abnormal and state-specific coexistence of wake-like and sleep-like EEG activity, even in the same brain regions (Flamand et al., 2018).

Another insight is offered by a different aspect of regional dissociation, meaning the observation of brain regions relatively spared by the massive increase in SWA power during episodes (bilateral precuneus and right supramarginal and bilateral angular gyri).

Patients with DOA might be predisposed to this state-specific dissociation, due to a trait-like abnormal distribution of power (relatively lower SWA power over centro-parietal brain regions), as shown in a previous hd-EEG study (Castelnovo et al., 2016). Notably, these trait-like abnormalities in SWA power could be detected also during REM sleep, possibly justifying the occasional description of similar state-dissociations during REM sleep (Bhat, Patel, Rosen, & Chokroverty, 2012; Futenma et al., 2022).

More specifically, the right supramarginal and bilateral angular gyri are cross-modal associative areas implicated in visuo-spatial attention, reorientation of attention towards relevant stimuli, and manipulation of mental representations (Pedrazzini & Ptak, 2019). All these functions are essential to patients in order to navigate through space during clinical episodes. Precuneus, is instead known to be involved in episodic memory, visuospatial processing, reflections upon selfhttps://en.wikipedia.org/wiki/Self_(psychology) (Cavanna & Trimble, 2006), and aspects of conscious experience independently from memory retrieval (Siclari et al., 2017). Thus, the relative decrease in SWA power, typically associated with unconscious states like slow wave sleep or coma, in these brain regions, supports the idea that consciousness reemerges during DOA episodes, although probably in an altered form, during clinical episodes. This hypothesis goes in line with growing evidence pointing to the presence of some form of mental activity during DOA episodes (Baldini et al., 2019; Castelnovo, Loddo, Provini, Miano, & Manconi, 2021; Oudiette et al., 2009). PTE analysis further supports this hypothesis, revealing an increase in integrated and differentiated connectivity from baseline to episodes, typical of wakefulness (Tononi, 2004).

Interestingly, SWA connectivity during baseline sleep displayed an asymmetric frontal right-dominant and antero-posterior pattern. This pattern recalls that observed by studies on slow wave traveling, an indirect measure of brain connectivity during slow wave sleep: larger slow waves are more likely to originate from the right hemisphere (Avvenuti et al., 2020) and to travel antero-posteriorly (Massimini, Huber, Ferrarelli, Hill, & Tononi, 2004). Notably, a bilateral involvement at the beginning of the episode, along with the major involvement of the left temporal lobe, seems to be an essential feature associated with DOA episodes, as in Ratti et al. (2018).

Furthermore, the all-brain and fine-grained connectivity analysis conducted in the source space in this current work allowed for the identification of specific out-flow hubs involved in DOA episodes. Curiously, these hubs mainly involved the ventromedial prefrontal cortex, the left temporal pole, and the left anterior insula, whose function seems to remain deactivated ("sleepier") during DOA episodes. Indeed, the ventromedial prefrontal cortex is thought to represent emotion and reward in decision making as well as facial emotion recognition, theory-of-mind ability processing self-relevant information (Dixon, Thiruchselvam, Todd, & Christoff, 2017; Hiser & Koenigs, 2018), functions that are likely shared with the left temporal pole (Olson, Plotzker, & Ezzyat, 2007). Similarly, the left anterior insula is activated by all valence categories of emotions, and is involved in social emotions, emotional awareness, and switching between the central executive network and the default mode network (Gu, Hof, Friston, & Fan, 2013; Lamm & Singer, 2010). Notably, the right insula was not involved in SWA connectivity (meaning that it is probably more 'active' during DOA episodes). Right insula is specifically involved in the processing of negative emotions (Gu et al., 2013), which are dominantly expressed during clinical behavioral events (Oudiette et al., 2011).

Overall, the knowledge of specific EEG dynamics during DOA episodes provides a plausible explanation for some of the observed behavioral and mental features associated with DOA episodes.

4.3. *Strengths, limitations and future directions*

Of note, we only captured confusional arousal and minor events and not sleep terrors or sleepwalking episodes. This is in line with data from the literature, which suggests that it is difficult to capture major events during vPSG recordings (Loddo et al., 2009). However, although some differences may exist between different DOA manifestations, it is known that they all belong to the same family of disorders and can also coexist in the same subject or family (Petit et al., 2015). Moreover, confusional arousal and minor episodes are those that pose greater issues of differential diagnosis with SHE in clinical practice (Derry, Harvey, Walker, Duncan, & Berkovic, 2009; Zucconi & Ferini-Strambi, 2000). Therefore, the analysis of minor events is essential for the development of objective methods and tools to support the diagnostic process.

The data reported came from the analysis of DOA episodes from one single subject, and therefore they cannot be generalized to the entire DOA population. It is possible that brain activity during clinical episodes varies from patient to patient, justifying different clinical subtypes and the heterogeneity of DOA semeiology. However, this case report clearly demonstrated that hd-EEG analysis of DOA episodes is feasible, and due to its high spatial and temporal resolution could reveal essential pieces of information to clarify these mysterious phenomena. Future studies should strive to collect DOA episodes in a fairly large clinical sample.

Last but not least, functional connectivity results, despite providing the first detailed insight into brain functioning during clinical DOA episodes, are undermined by the lack of literature on physiological data during both sleep and wakefulness. Our case report calls for the urgent need of studies to cover these gaps in our understanding of brain networks across different brain states.

5. Conclusions

DOA events analyzed for this case report were associated with a drastic decrease of sigma activity compared to average slow wave sleep, likely reflecting a suppression of sleep spindles, as in physiological arousal. On the other hand, all other frequency bands displayed a diffuse absolute increase, suggesting a divergence with normal arousal. Interestingly, in the SWA range, a centro-posterior region encompassing precuneus, paracentral parietal lobule and right supramarginal and angular lobule, seemed to be significantly less involved by this massive increase in power. Functional connectivity in the SWA range displayed a clearcut switch from poorly to highly integrated networks where bilateral orbitofrontal and left ventro-medial temporal lobe were the main output hubs.

Overall, these results parallel the observable behavioral expression of DOA episodes, support the idea that DOA are the expression of peculiar brain states, possibly intermediate between sleep and wakefulness, and point to key patterns subserving a partial re-emergence of consciousness.

We envisage that the systematic analysis of DOA episodes and of other sleep events in potential differential diagnosis, such as SHE, will foster the development of specific tools to support the diagnostic process in most difficult and complex cases.

Open practices

The study in this article earned an Open Data – Protected Access badge for transparent practices. Materials and data for the study are available at https://doi.org/10.5281/zenodo.6501824.

Funding

This study was supported by an ABREOC grant (Advisory Board of Scientific Research of the Ente Ospedaliero Cantonale).

Color statement

Color should be used for all figures in print.

Transparency statement

We report all data exclusions (if any), all inclusion/exclusion criteria, whether inclusion/exclusion criteria were established prior to data analysis, all manipulations and all measures in the study.

Data availability statement

The EEG data that support the findings of this study are openly available at https://doi.org/10.5281/zenodo.6501824.

Code availability statement

The code that supports the findings of this study is openly available at https://github.com/AnnaCastelnovo/sleep-EOC.git.

Pre-registration

No part of the study procedures was pre-registered prior to the research being conducted.

No part of the study analyses was pre-registered prior to the research being conducted.

Credit author statement

Anna Castelnovo: Conceptualization, Methodology, Investigation, Project administration, Funding acquisition, Software, Formal analysis, Data Curation, Visualization, Writing- Original draft preparation, Reviewing and Editing. **Julian Amacker:**

Software, Formal analysis, Visualization, Reviewing and Editing. **Massimo Maiolo:** Software, Formal analysis, Visualization, Reviewing and Editing. **Ninfa Amato:** Software, Funding acquisition, Reviewing and Editing. **Matteo Pereno:** Investigation, **Silvia Riccardi:** Reviewing and Editing, **Andrea Danani:** Methodology, Reviewing and Editing, **Simone Ulzega:** Software, Formal analysis, Visualization, Reviewing and Editing. **Mauro Manconi:** Resources, Supervision, Funding acquisition, Reviewing and Editing.

Declaration of competing interest

None to declare.

Acknowledgments

We are deeply grateful to the patient and his family. We also thank the Advisory Board of Scientific Research organized by the Ente Ospedaliero Cantonale (ABREOC) that funded data collection.

Supplementary data

Supplementary data to this article can be found online at https://doi.org/10.1016/j.cortex.2022.05.021.

REFERENCES

Avvenuti, G., Handjaras, G., Betta, M., Cataldi, J., Imperatori, L. S., Lattanzi, S., et al. (2020). Integrity of corpus callosum is essential for the cross-hemispheric propagation of sleep slow waves: A high-density eeg study in split-brain patients. *Journal of Neuroscience, 40*(29), 5589–5603. https://doi.org/10.1523/JNEUROSCI.2571-19.2020

Baldini, T., Loddo, G., Sessagesimi, E., Mignani, F., Cirignotta, F., Mondini, S., et al. (2019). Clinical features and pathophysiology of disorders of arousal in adults: A window into the sleeping brain. *The Florida Nurse, 10*(MAY), 1–9. https://doi.org/10.3389/fneur.2019.00526

Bassetti, C., Vella, S., Donati, F., & Wielepp, P. (2000). SPECT during sleepwalking. *The Lancet, 356*, 484–485.

Berry, R. B., Brooks, R., Gamaldo, C., Harding, S. M., Lloyd, R. M., Quan, S. F., … Vaughn, B. V. (2020). AASM Scoring Manual Updates for 2017 (Version 2.4). *Journal of Clinical Sleep Medicine, 13*(5), 665–666.

Bhat, S., Patel, D., Rosen, D., & Chokroverty, S. (2012). A case of a confusional arousal arising from REM sleep. *Sleep Medicine, 13*(3), 317–318. https://doi.org/10.1016/j.sleep.2011.10.028

Castelnovo, A., Loddo, G., Provini, F., & Manconi, M. (2021). Frequent, complex and vivid dream-like/hallucinatory experiences during NREM sleep parasomnia episodes. *Sleep Medicine, 82*, 61–64. https://doi.org/10.1016/J.SLEEP.2021.03.032

Castelnovo, A., Loddo, G., Provini, F., Miano, S., & Manconi, M. (2021). Mental activity during episodes of sleepwalking, night terrors or confusional arousals: Differences between children and adults. *Nature and Science of Sleep, 13*, 829–840. https://doi.org/10.2147/NSS.S309868

Castelnovo, A., Lopez, R., Proserpio, P., Nobili, L., & Dauvilliers, Y. (2018). NREM sleep parasomnias as disorders of sleep-state dissociation. *Nature Reviews. Neurology, 14*(8), 470–481. https://doi.org/10.1038/s41582-018-0030-y

Castelnovo, A., Riedner, B. A., Smith, R. F., Tononi, G., Boly, M., & Benca, R. M. (2016). Scalp and source power topography in sleepwalking and sleep terrors: A high-density EEG study. *Sleep, 39*(10), 1815–1825. https://doi.org/10.5665/sleep.6162

Cavanna, A. E., & Trimble, M. R. (2006). The precuneus: A review of its functional anatomy and behavioural correlates. *Brain, 129*(Pt 3), 564–583. https://doi.org/10.1093/brain/awl004

Delorme, A., & Makeig, S. (2004). Eeglab: An open source toolbox for analysis of single-trial EEG dynamics including independent component analysis. *Journal of Neuroscience Methods, 134*(1), 9–21. https://doi.org/10.1016/j.jneumeth.2003.10.009

Derry, C. P., Harvey, A. S., Walker, M. C., Duncan, J. S., & Berkovic, S. F. (2009). NREM arousal parasomnias and their distinction from nocturnal frontal lobe epilepsy: A video EEG analysis. *Sleep, 32*(12), 1637–1644. https://doi.org/10.1093/sleep/32.12.1637

Desjardins, M.È., Carrier, J., Lina, J. M., Fortin, M., Gosselin, N., Montplaisir, J., et al. (2017). EEG functional connectivity prior to sleepwalking: Evidence of interplay between sleep and wakefulness. *Sleep, 40*(4), 1–8. https://doi.org/10.1093/sleep/zsx024

Destrieux, C., Fischl, B., Dale, A., & Halgren, E. (2010). Automatic parcellation of human cortical gyri and sulci using standard anatomical nomenclature. *NeuroImage, 53*(1), 1–15. https://doi.org/10.1016/j.neuroimage.2010.06.010

Dixon, M. L., Thiruchselvam, R., Todd, R., & Christoff, K. (2017). Emotion and the prefrontal cortex: An integrative review. *Psychological Bulletin, 143*(10), 1033–1081. https://doi.org/10.1037/bul0000096

Espa, F., Ondze, B., Deglise, P., Billiard, M., & Besset, A. (2000). Sleep architecture, slow wave activity, and sleep spindles in adult patients with sleepwalking and sleep terrors. *Clinical Neurophysiology, 111*(5), 929–939. https://doi.org/10.1016/S1388-2457(00)00249-2

Fernandez, L. M. J., & Lüthi, A. (2020). Sleep spindles: Mechanisms and functions. *Physiological Reviews, 100*, 805–868. https://doi.org/10.1152/physrev.00042.2018

Flamand, M., Boudet, S., Lopes, R., Vignal, J. P., Reyns, N., Charley-Monaca, C., et al. (2018). Confusional arousals during non-rapid eye movement sleep: Evidence from intracerebral recordings. *Sleep, 41*(10), 1–11. https://doi.org/10.1093/sleep/zsy139

Fraschini, M., Demuru, M., Crobe, A., Marrosu, F., Stam, C. J., & Hillebrand, A. (2016). The effect of epoch length on estimated EEG functional connectivity and brain network organisation. *Journal of Neural Engineering, 13*(3), 036015. https://doi.org/10.1088/1741-2560/13/3/036015

Futenma, K., Inoue, Y., Saso, A., Takaesu, Y., Yamashiro, Y., & Matsuura, M. (2022). Three cases of parasomnias similar to sleep terrors occurring during sleep-wake transitions from REM sleep. *Journal of Clinical Sleep Medicine, 18*(2), 669–675. https://doi.org/10.5664/jcsm.9666

Greenblatt, R. E., Pflieger, M. E., & Ossadtchi, A. E. (2012). Connectivity measures applied to human brain electrophysiological data. *Journal of Neuroscience Methods, 207*(1), 1–16. https://doi.org/10.1016/j.jneumeth.2012.02.025

Gu, X., Hof, P. R., Friston, K. J., & Fan, J. (2013). Anterior insular cortex and emotional awareness. *Journal of Comparative Neurology, 521*(15), 3371–3388. https://doi.org/10.1002/cne.23368

Guilleminault, C., Poyares, D., Abat, F., & Palombini, L. (2001). Sleep and wakefulness in somnambulism: A spectral analysis

study. *Journal of Psychosomatic Research*, 51(2), 411–416. https://doi.org/10.1016/S0022-3999(01)00187-8

Hillebrand, A., Tewarie, P., Van Dellen, E., Yu, M., Carbo, E. W. S., Douw, L., et al. (2016). Direction of information flow in large-scale resting-state networks is frequency-dependent. In *Proceedings of the national academy of sciences of the United States of America*. https://doi.org/10.1073/pnas.1515657113

Hiser, J., & Koenigs, M. (2018). The multifaceted role of the ventromedial prefrontal cortex in emotion, decision making, social cognition, and psychopathology. *Biological Psychiatry, 83*(8), 638–647. https://doi.org/10.1016/j.biopsych.2017.10.030

Ingravallo, F., Poli, F., Gilmore, E. V., Pizza, F., Vignatelli, L., Schenck, C. H., et al. (2014). Sleep-related violence and sexual behavior in sleep: A systematic review of medical-legal case reports. *Journal of Clinical Sleep Medicine, 10*(8), 927–935. https://doi.org/10.5664/jcsm.3976

Jaar, O., Pilon, M., Carrier, J., Montplaisir, J., & Zadra, A. (2010). Analysis of slow-wave activity and slow-wave oscillations prior to somnambulism. *Sleep, 33*(11), 1511–1516. https://doi.org/10.1093/sleep/33.11.1511

Januszko, P., Niemcewicz, S., Gajda, T., Wołyńczyk-Gmaj, D., Piotrowska, A. J., Gmaj, B., et al. (2016). Sleepwalking episodes are preceded by arousal-related activation in the cingulate motor area: EEG current density imaging. *Clinical Neurophysiology, 127*(1), 530–536. https://doi.org/10.1016/j.clinph.2015.01.014

Lamm, C., & Singer, T. (2010). The role of anterior insular cortex in social emotions. *Brain Structure & Function, 214*(5–6), 579–591. https://doi.org/10.1007/s00429-010-0251-3

Lobier, M., Siebenhühner, F., Palva, S., & Palva, J. M. (2014). Phase transfer entropy: A novel phase-based measure for directed connectivity in networks coupled by oscillatory interactions. *NeuroImage, 85*(Pt 2), 853–872. https://doi.org/10.1016/j.neuroimage.2013.08.056

Loddo, G., Sessagesimi, E., Mignani, F., Cirignotta, F., Mondini, S., Licchetta, L., et al. (2009). Specific motor patterns of arousal disorders in adults: A video-polysomnographic analysis of 184 episodes. *Sleep, 32*(12), 936–940. https://doi.org/10.1093/sleep/32.12.1637

Loddo, G., Sessagesimi, E., Mignani, F., Cirignotta, F., Mondini, S., Licchetta, L., et al. (2018). Specific motor patterns of arousal disorders in adults: A video-polysomnographic analysis of 184 episodes. *Sleep Medicine, 41*, 102–109. https://doi.org/10.1016/j.sleep.2017.08.019

Massimini, M., Huber, R., Ferrarelli, F., Hill, S., & Tononi, G. (2004). The sleep slow oscillation as a traveling wave. *Journal of Neuroscience, 24*(31), 6862–6870. https://doi.org/10.1523/JNEUROSCI.1318-04.2004

Maureen, C. (2010). An empirical evaluation of free BEM solvers for accurate M/EEG forward modeling. *The Florida Nurse*, (Event Abstract). https://doi.org/10.3389/conf.fnins.2010.06.00065

Mwenge, B., Brion, A., Uguccioni, G., & Arnulf, I. (2013). Sleepwalking: Long-term home video monitoring. *Sleep Medicine, 14*(11), 1126–1228. https://doi.org/10.1016/j.sleep.2013.04.027

Naitoh, P., Antony-Baas, V., Muzet, A., & Ehrhart, J. (1982). Dynamic relation of sleep spindles and K-complexes to spontaneous phasic arousal in sleeping human subjects. *Sleep, 5*(1), 58–72. https://doi.org/10.1093/sleep/5.1.58

Nakamura, B. J., Ebesutani, C., Bernstein, A., & Chorpita, B. F. (2009). A psychometric analysis of the child behavior checklist DSM-oriented scales. *Journal of Psychopathology and Behavioral Assessment, 109*, 103834. https://doi.org/10.1007/s10862-008-9119-8

Nichols, T. E., Holmes, A. P., & Human Brain Mapping. (2001). Nonparametric permutation tests for functional neuroimaging: A primer with examples. *Human Brain Mapping, 15*, 1–25.

Nolte, G., Bai, O., Wheaton, L., Mari, Z., Vorbach, S., & Hallett, M. (2004). Identifying true brain interaction from EEG data using the imaginary part of coherency. *Clinical Neurophysiology, 115*(10), 2292–2307. https://doi.org/10.1016/j.clinph.2004.04.029

Olson, I. R., Plotzker, A., & Ezzyat, Y. (2007). The enigmatic temporal pole: A review of findings on social and emotional processing. *Brain, 130*(Pt 7), 1718–1731. https://doi.org/10.1093/brain/awm052

Oudiette, D., Constantinescu, I., Leclair-Visonneau, L., Vidailhet, M., Schwartz, S., & Arnulf, I. (2011). Evidence for the re-enactment of a recently learned behavior during sleepwalking. *PLoS ONE, 6*(3), 1–8. https://doi.org/10.1371/journal.pone.0018056

Oudiette, D., Leu, S., Pottier, M., Buzare, M. A., Brion, A., & Arnulf, I. (2009). Dreamlike mentations during sleepwalking and sleep terrors in adults. *Sleep, 32*(12), 1621–1627. https://doi.org/10.1093/sleep/32.12.1621

Pedrazzini, E., & Ptak, R. (2019). Damage to the right temporoparietal junction, but not lateral prefrontal or insular cortex, amplifies the role of goal-directed attention. *Scientific Reports, 9*(1), 306. https://doi.org/10.1038/s41598-018-36537-3

Pereda, E., Quiroga, R. Q., & Bhattacharya, J. (2005). Nonlinear multivariate analysis of neurophysiological signals. *Progress in Neurobiology, 77*(1–2), 1–37. https://doi.org/10.1016/j.pneurobio.2005.10.003

Perrault, R., Carrier, J., Desautels, A., Montplaisir, J., & Zadra, A. (2014). Electroencephalographic slow waves prior to sleepwalking episodes. *Sleep Medicine, 15*(12), 1468–1472. https://doi.org/10.1016/j.sleep.2014.07.020

Peter-Derex, L., Magnin, M., & Bastuji, H. (2015). Heterogeneity of arousals in human sleep: A stereo-electroencephalographic study. *NeuroImage, 123*, 229–244. https://doi.org/10.1016/j.neuroimage.2015.07.057

Petit, D., Pennestri, M. H., Paquet, J., Desautels, A., Zadra, A., Vitaro, F., et al. (2015). Childhood sleepwalking and sleep terrors: A longitudinal study of prevalence and familial aggregation. *JAMA Pediatrics, 169*(7), 653–658. https://doi.org/10.1001/jamapediatrics.2015.127

Ratti, P. L., Amato, N., David, O., & Manconi, M. (2018). A high-density polysomnographic picture of disorders of arousal. *Sleep, 41*(11), 1–3. https://doi.org/10.1093/sleep/zsy162

Richards, J. E., Sanchez, C., Phillips-Meek, M., & Xie, W. (2016). A database of age-appropriate average MRI templates. *NeuroImage, 124*(Pt B), 1254–1259. https://doi.org/10.1016/j.neuroimage.2015.04.055

Rocha, A., & Arnulf, I. (2020). NREM parasomnia as a dream enacting behavior. *Sleep Medicine, 75*, 103–105. https://doi.org/10.1016/j.sleep.2020.02.024

Sarasso, S., Pigorini, A., Proserpio, P., Gibbs, S. A., Massimini, M., & Nobili, L. (2014). Fluid boundaries between wake and sleep: Experimental evidence from Stereo-EEG recordings. *Archives Italiennes de Biologie, 152*(2–3), 169–177. https://doi.org/10.12871/0002982920142311

Schenck, C. H., Pareja, J. A., Patterson, A. L., & Mahowald, M. W. (1998). Analysis of polysomnographic events surrounding 252 slow-wave sleep arousals in thirty-eight adults with injurious sleepwalking and sleep terrors. *Journal of Clinical Neurophysiology, 15*(2), 159–166. https://doi.org/10.1097/00004691-199803000-00010

Sforza, E., Jouny, C., & Ibanez, V. (2000). Cardiac activation during arousal in humans: Further evidence for hierarchy in the arousal response. *Clinical Neurophysiology, 111*, 1611–1619. https://doi.org/10.1016/S1388-2457(00)00363-1

Siclari, F., Baird, B., Perogamvros, L., Bernardi, G., LaRocque, J. J., Riedner, B., et al. (2017). The neural correlates of dreaming. *Nature Neuroscience, 20*(6), 872–878. https://doi.org/10.1038/nn.4545

Tadel, F., Baillet, S., Mosher, J. C., Pantazis, D., & Leahy, R. M. (2011). Brainstorm: A user-friendly application for MEG/EEG analysis. *Computational Intelligence and Neuroscience*. https://doi.org/10.1155/2011/879716

Terzaghi, M., Sartori, I., Tassi, L., Didato, G., Rustioni, V., LoRusso, G., et al. (2009). Evidence of dissociated arousal states during nrem parasomnia from an intracerebral neurophysiological study. *Sleep, 32*(3), 409–412. https://doi.org/10.1093/sleep/32.3.409

Terzaghi, M., Sartori, I., Tassi, L., Rustioni, V., Proserpio, P., Lorusso, G., et al. (2012). Dissociated local arousal states underlying essential clinical features of non-rapid eye movement arousal parasomnia: An intracerebral stereo-electroencephalographic study. *Journal of Sleep Research, 21*(5), 502–506. https://doi.org/10.1111/j.1365-2869.2012.01003.x

Tononi, G. (2004). An information integration theory of consciousness. *BMC Neuroscience, 5*, 42. https://doi.org/10.1186/1471-2202-5-42

Tzourio-Mazoyer, N., Landeau, B., Papathanassiou, D., Crivello, F., Etard, O., Delcroix, N., et al. (2002). Automated anatomical labeling of activations in SPM using a macroscopic anatomical parcellation of the MNI MRI single-subject brain. *NeuroImage, 14*(5), 391–398. https://doi.org/10.1006/nimg.2001.0978

Uguccioni, G., Golmar, J. L., Noël de Fontréaux, A., Leu-Semenescu, S., Brion, A., & Arnulf, I. (2013). Fight or flight? Dream content during sleepwalking/sleep terrors vs rapid eye movement sleep behavior disorder. *Sleep Medicine, 14*(5), 391–394. https://onlinelibrary.wiley.com/doi/10.1111/jsr.12219 10.1016/j.sleep.2013.01.014.

Zadra, A., Desautels, A., Petit, D., & Montplaisir, J. (2013). Somnambulism: Clinical aspects and pathophysiological hypotheses. The. *Lancet Neurology, 12*(3), 285–294. https://doi.org/10.1016/S1474-4422(12)70322-8

Zadra, A., & Nielsen, T. (1998). Topographical EEG mapping in a case of recurrent sleep terrors. *Dreaming, 8*, 67–74. https://doi.org/10.1023/B:DREM.0000005897.62698

Zadra, A., Pilon, M., Joncas, S., Rompré, S., & Montplaisir, J. (2004). Analysis of postarousal EEG activity during somnambulistic episodes. *Journal of Sleep Research, 13*(3), 279–284. https://doi.org/10.1111/j.1365-2869.2004.00404.x

Zucconi, M., & Ferini-Strambi, L. (2000). NREM parasomnias: Arousal disorders and differentiation from nocturnal frontal lobe epilepsy. *Clinical Neurophysiology*, (Suppl 2), S129–S135. https://doi.org/10.1016/S1388-2457(00)00413-2